THE JOURNAL OF BIOLOGICAL CHEMISTRY
Vol. 271, No. 39, Issue of September 27, pp. 23836–23841, 1996

Printed in U.S.A.

Structural and Functional Aspects of Chloride Binding to *Alteromonas haloplanctis* α-Amylase*

(Received for publication, June 5, 1996, and in revised form, July 12, 1996)

Georges Feller‡, Olivier le Bussy, Corinne Houssier, and Charles Gerday

From the Laboratory of Biochemistry, Institute of Chemistry B6, University of Liège, B-4000 Liège, Belgium

Chloride is the allosteric effector of vertebrate pancreatic and salivary α-amylases and of the bacterial α-amylase from *Alteromonas haloplanctis*. Activation experiments of *A. haloplanctis* α-amylase by several monovalent anions show that a negative charge, not restricted to that of Cl^-, is essential for the amylolytic reaction. Engineering of the chloride binding site reveals that a basic residue is an essential component of the site. The mutation K337R alters the Cl^--binding properties, whereas the mutation K337Q produces an active, chloride-independent enzyme. Comparison of the K_d values for Cl^- in three homologous α-amylases also indicates that the binding affinity is dependent on the chloride coordination mode by this basic residue. Analysis of substrate and chloride binding according to the allosteric kinetic model shows that the chloride effector is not involved in substrate binding. By contrast, the pH dependence of activity and experiments of chemical modifications and Ca^{2+} inhibition show that the chloride ion is responsible for the pK_a shift of catalytic groups and interacts with active site carboxyl groups.

α-Amylases (α-1,4-glucan-4-glucanohydrolase, EC 3.2.1.1) are widely distributed in microorganisms, plants, and animals. They catalyze the hydrolysis of internal α(1,4)-glycosidic bonds with net retention of the anomeric configuration in starch, amylose, amylopectin, glycogen, and other polysaccharides through multiple attacks toward the nonreducing end (1). Recently, the high resolution x-ray structure of α-amylases from *Aspergillus niger* (2), from *Aspergillus oryzae* (3), from human (4) and porcine (5, 6) pancreas, from human salivary glands (7), from barley seeds (8), and from *Bacillus licheniformis* (9) have been published. All are monomers of about 50 kDa and exhibit a central main domain A formed by a $(\beta/\alpha)_8$-barrel, a small β-pleated domain B protruding between β_3 and α_3 and a C-terminal globular domain C consisting of a Greek key motif. α-Amylase requires at least one tightly bound calcium ion for its structural integrity and for enzymatic activity (1, 10, 11). A general mechanism for glycosidases retaining the anomeric configuration is now recognized that involves a double displacement mechanism and a glycosyl-enzyme intermediate (12, 13). A pair of carboxylic acids is found at the active site; one acts as a general acid and a general base while the other behaves as a nucleophile favoring the stabilization of an oxocarbonium ion and the diffusion of the leaving group. In α-amylases, the mechanism seems to require a third carboxyl group (14). Several experimental results support the formation of a covalent intermediate, namely a β-carboxyl-acetal ester (15, 16), whereas crystal structures of the complex of glycosidases with carbohydrate inhibitors favor an oxocarbonium ion transition state (17–19).

Historically, porcine pancreatic α-amylase was the first enzyme found to be modulated by chloride. Binding of one chloride ion at a specific site induces the allosteric activation of α-amylase (20, 21). Chloride activation has been demonstrated in mammalian pancreatic and salivary α-amylases (1) and in the structurally related bacterial enzyme from *Alteromonas haloplanctis* (22, 23) whereas most microbial α-amylases seem chloride independent (24). With the recent description of the refined molecular structure of pancreatic and salivary α-amylases, it is now possible to investigate the function of chloride in catalysis. The results presented here show that the monovalent ion is responsible for the pK_a shift of catalytic groups and interacts with active site carboxyl groups. The chloride binding site was also engineered in order to produce an active, chloride-independent enzyme.

EXPERIMENTAL PROCEDURES

Sources—The origin and culture conditions of the psychrophile *A. haloplanctis* A23, as well as the purification protocol of the secreted α-amylase, have been described previously (22, 23). *Thermomonospora curvata* CCM 3352 was from the Czech Collection of Microorganisms (Brno). Halide sodium salts were from Merck (Suprapur), and Hepes was from Sigma (SigmaUltra). Crystallographic coordinates for pig pancreatic α-amylase (18) were obtained from the Brookhaven Protein Data Bank under filename 1PPI.

Enzyme Assays and Kinetics—Standard assay was carried out at 25 °C with the α-amylase EPS kit (Boehringer) using 3.5 mM 4-nitrophenyl-α-D-maltoheptaoside-4,6-O-ethylidene (EPS)[1] as substrate and excess (23 units/ml) of α-glucosidase as coupling enzyme in 100 mM Hepes, 50 mM NaCl, 10 mM $MgCl_2$, pH 7.1. Activities toward the synthetic substrate were recorded in a thermostated Uvikon 860 spectrophotometer (Kontron) and were calculated on the basis of an absorption coefficient for 4-nitrophenoside ion of 8,980 M^{-1} cm^{-1} at 405 nm (25). The amylolytic activity was also determined by the dinitrosalicylic acid method (26) using 1% soluble starch (Sigma) as substrate in the above mentioned buffer.

The enzyme concentrations were determined by the Coomassie Protein Assay Reagent (Pierce). The kinetic parameters k_{cat} and K_m were determined by the initial velocity method using a nonlinear regression computer fit of the saturation curves. The pH dependence of k_{cat} and K_m was analyzed using starch as substrate in a buffer mixture containing 30 mM each acetate, Hepes, Mes, Ches, and various NaCl concentrations. The optimum pH for the activity of recombinant α-amylases was determined in 50 mM Mes, 50 mM Bes.

Anion and Ca^{2+} Titration of Apo-α-Amylase—Cl^--free α-amylase was prepared by dialysis or by gel filtration on a Sephadex G25 column

* This work was supported by E U Network Contract ERB-CHRXCT94021 and by the "Ministère de l'Education, de la Recherche et de la Formation" (ARC 93/98-170). The costs of publication of this article were defrayed in part by the payment of page charges. This article must therefore be hereby marked "*advertisement*" in accordance with 18 U.S.C. Section 1734 solely to indicate this fact.

‡ To whom correspondence should be addressed. Tel.: 32-41663343; Fax: 32-41663364.

[1] The abbreviations used are: EPS, 4-nitrophenyl-α-D-maltoheptaoside-4,6-*O*-ethylidene; Mes, 2-(*N*-morpholino)ethanesulfonic acid; Ches, 2-(*N*-cyclohexylamino)ethanesulfonic acid; Bes, *N*,*N*-bis(2-hydroxyethyl)-2-aminoethanesulfonic acid; WRK, Woodward's Reagent K or *N*-ethyl-5-phenylisoxazolium-3′-sulfonate.

eluted with 25 mM Hepes-NaOH, pH 7.0. The dissociation constants for Cl^- and other anions were calculated from activation curves generated by NaCl titration (or the corresponding sodium salt) in the EPS reaction mixture except that the buffer was replaced by 25 mM Hepes-NaOH, pH 7.1. Starch was used as substrate for Cl^- titration of *T. curvata* α-amylase. The saturation curves were computer-fitted by a nonlinear regression analysis of the Hill equation in the following form,

$$v = k_{cat}[A]^{n_H}/K_d + [A]^{n_H} \quad \text{(Eq. 1)}$$

where [A] is the anion concentration and n_H is the Hill coefficient.

Apo α-amylase (Cl^-, Ca^{2+} free) was prepared by overnight dialysis of the native enzyme against 25 mM Hepes-NaOH, 5 mM EGTA, pH 7.0. Activation kinetics by calcium titration were performed in 25 mM Hepes-NaOH, 5 mM EGTA, 1% starch, pH 7.0, and various NaCl concentrations. The desired free Ca^{2+} concentration was set by addition of 30 mM calcium acetate, according to a program described elsewhere (27).

Chemical Modification by WRK—α-amylase (0.1 μM) in 200 mM Hepes-NaOH, pH 7.1, was inactivated by 2–10 mM WRK at 0 °C. Aliquots of inactivation mixture and of controls were withdrawn at time intervals, and the residual activity was measured using EPS as substrate. Inactivation was carried out in the presence of various concentrations of NaCl, NaBr, NaI, starch, and EPS. The lower reagent concentrations led to incomplete inactivation (with a residual activity V_∞), and data were fitted to the following equation (28):

$$V_t - V_\infty = (V_0 - V_\infty)e^{-kt} \quad \text{(Eq. 2)}$$

Site-directed Mutagenesis—Mutations K(AAA)337R(AGA) and K337Q(CAA) in the chloride binding site were introduced by inverse polymerase chain reaction (29). The gene of *A. haloplanctis* α-amylase (22) cloned upstream of the *LacZ* promoter of pUC12 was used as template. This construction is devoid of the C-terminal peptide cleaved by the wild strain following α-amylase secretion.[2] The mutating sense primers were designed by positioning 3 codons in 5′ from the codon to be mutated and 5 codons in 3′ from the mutation. Silent antisense primers were 24 nucleotides in length. Synthetic oligonucleotides were from Pharmacia Biotech and Eurogentec (Belgium). Polymerase chain reaction amplification conditions by $Vent_R$ DNA polymerase (New England Biolabs) were as described previously (30). Mutants were generated by insertion of the mutated *Acc*I-*Ava*I fragment (0.34 kilobases) in the original plasmid, and the sequence of the construction was checked on a Pharmacia ALF DNA sequencer. The recombinant α-amylase and the mutant enzymes were purified from the culture supernatant of *Escherichia coli* RR1 using the protocol developed for the wild type α-amylase except that acetone precipitation (between 45% and 70% (v/v)) was required before the first chromatographic step.

RESULTS

Cl^- and Monovalent Ion Binding—Removal of Cl^- either by dialysis or gel filtration results in the reversible inactivation of *A. haloplanctis* α-amylase. As shown in Table I, the enzyme can be fully reactivated by chloride but also by Br^- and to a lesser extent by I^- and some other monovalent anions. The small fluoride ion is almost ineffective for α-amylase activation, whereas the divalent sulfate anion has no activation capacity. Essentially similar results were obtained using either starch or EPS as substrate. The apparent dissociation constants K_d were determined by activation kinetics (Fig. 1*A*) and are given in Table I. It has been previously shown that activation kinetics of hog α-amylase and direct binding measurements using ^{36}Cl give identical results (20). Hill coefficient (n_H) for each titration of *A. haloplanctis* α-amylase was ~1, confirming that only one anion is bound during activation. Fig. 1*B* illustrates the close relation between halide ion size and the enzyme binding affinity, with iodide displaying the optimal binding value. Interestingly, the polyatomic NO_3^- and ClO_3^- anions bind more strongly than halides. However, there is no direct relation between the K_d values and the activation capacity shown in Table I.

A. haloplanctis is a psychrophilic marine bacterium; taking into account the dissociation constants at 5 °C (1.6, 0.35, and 0.25 mM for Cl^-, Br^-, and I^-, respectively) and the anion concentrations in sea water (536 mM, 813 μM, and 4 nM for Cl^-, Br^-, and I^- respectively), one can calculate that the α-amylase-chloride complex is the dominant species (99%) in the natural environment on the basis of a simple competition of halides for the same site.

TABLE I
Activation capacity of various anions (at saturation, starch as substrate) on the amylolytic activity of A. haloplanctis α-amylase and their apparent dissociation constants

Anion	Relative activity	K_d
	%	mM
Cl^-	100	5.9
Br^-	98	2.8
NO_2^-	53	11.4
$HCOO^-$	52	52
I^-	48	2.3
NO_3^-	45	1.9
ClO_3^-	35	1.2
CNO^-	31	46
N_3^-	28	41
SCN^-	26	33
CH_3COO^-	12	219
F^-	0.8[a]	20
SO_4^{2-}	0.3[b]	
None	0.3[b]	

[a] 2.1% at pH 6.0.
[b] 10 μM chloride contamination in reagents.

Effect of Cl^- on the Amylolytic Reaction—The saturation curves of *A. haloplanctis* α-amylase by the natural and the synthetic substrates in the presence of saturating and subsaturating Cl^- concentrations are shown in Fig. 2 in the form of linear Hanes plots. These plots indicate that the K_m value for both substrates remains independent of Cl^- concentration. No significant variations of K_m occur when I^-, NO_2^-, NO_3^-, or CNO^- are the effectors. A kinetic model of the allosteric activation of *A. haloplanctis* α-amylase by chloride is shown in Fig. 3.

The following rate equation can be derived from this model:

$$v_0 = k_2[ESCl]$$
$$= k_2E_0[S][Cl]/([S][Cl] + K'_S[Cl] + K'_d[S] + K'_SK_d) \quad \text{(Eq. 3)}$$

The results of substrate titrations (at 50, 5, and 2 mM NaCl; K_m, EPS = 174 ± 8 μM; k_{cat} = 788 ± 8 s^{-1}) and of chloride titrations (at 3, 0.4, and 0.1 mM EPS; K_d = 5.9 ± 0.2 mM; k_{cat} = 854 ± 11 s^{-1}) have been analyzed simultaneously by Equation 3 using a non-linear regression analysis. Results define a surface between the orthogonal axis ([S], v_0, [Cl]). The computed kinetic and binding parameters are given in Table II according to the constraints imposed. If $K_d = K'_d$ (assuming that substrate and chloride binding are independent, therefore $K_S = K'_S$ in a system at equilibrium), the computed parameters are in excellent agreement with experimental values. When K_d and K'_d are solved independently, the computed dissociation constants for Cl^- are not significantly different; in addition K'_S and k_2 remain constant. By contrast, the system cannot be solved assuming that chloride is required for substrate binding ([ES] = 0).

The pH dependence of starch hydrolysis was also studied at saturating and subsaturating Cl^- concentrations. The K_m values were constant over the pH range examined. As shown in Fig. 4, *A* and *B*, the optimum pH and both acidic and alkaline pK_{app} are shifted toward the alkaline range when α-amylase is saturated by Cl^-. All anions studied in Table I induce the same shift at saturating concentration ($\Delta_{pHopt} \approx 1.2$) with the exception of acetate ($\Delta_{pHopt} \approx 0.8$) and of F^- for which no pH shift has been recorded. The bell-shaped pH dependence of k_{cat} can

[2] G. Feller, manuscript in preparation.

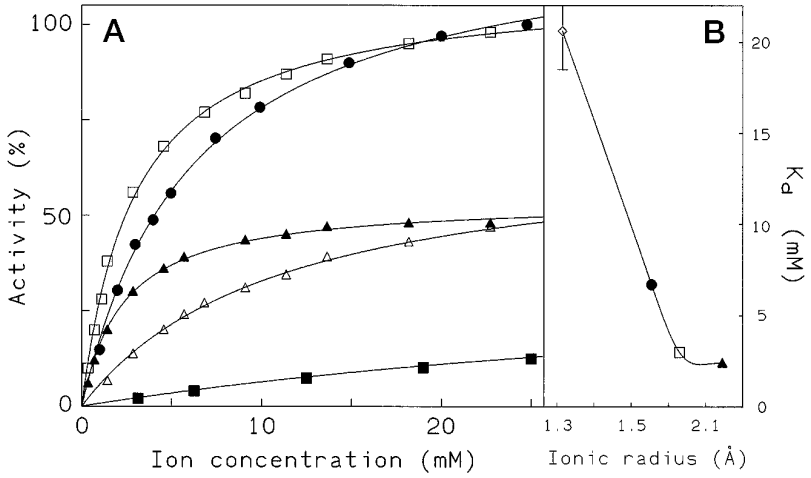

FIG. 1. **Activation of *A. haloplanctis* α-amylase by various monovalent anions.** *A*, activation by Cl^- (●), Br^- (□), I^- (▲), NO_2^- (△), and $HCOO^-$ (■) using EPS as substrate. *B*, apparent dissociation constants K_d for halides (*symbols* as in *A*) including F^- (◇).

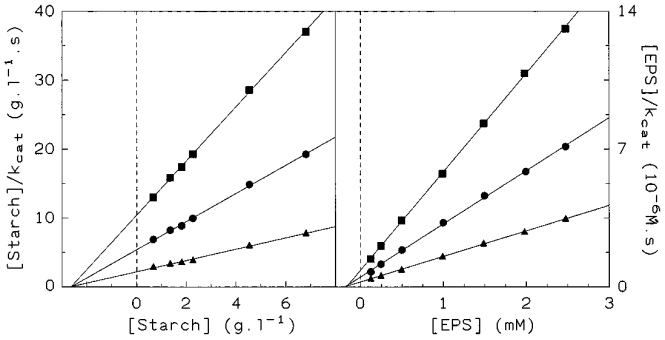

FIG. 2. **Activation of starch and EPS hydrolysis by chloride.** Hanes plots ($y = 0, x = -K_m$) of the α-amylase saturation curves by both substrates in the presence of 2 mM (■), 5 mM (●), and 50 mM (▲) NaCl show the increase of k_{cat} upon Cl^- binding and the constant K_m values.

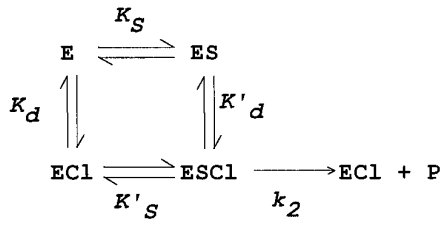

FIG. 3. **Allosteric activation of α-amylase by chloride.** *E*, *S*, *P*, and *Cl* refer to enzyme, substrate, product, and chloride, respectively; K_d and K'_d are the dissociation constants between chloride and the free enzyme or the enzyme-substrate complex, respectively; K_S and K'_S are the dissociation constants between the substrate and the free enzyme or the enzyme-chloride complex, respectively; k_2 is the hydrolytic rate constant.

be satisfactorily fitted with theoretical curves derived from the three-proton model proposed for mammalian pancreatic α-amylases (31, 32). Fig. 4*C* indicates that the chloride-induced alkaline shift of pK_2 and pK_3 approximates the chloride binding curve while the pK_1 value (~4.2) remains unaffected.

Interactions between Ca^{2+} and Cl^- Binding—α-Amylases bind one calcium ion with high affinity at a specific site. Excess of Ca^{2+} results in the binding of a second calcium ion by active site carboxylates and inhibits α-amylase activity (33). *A. haloplanctis* α-amylase is reversibly inactivated following Ca^{2+} removal by EGTA. Fig. 5 illustrates the Ca^{2+}-induced activation of the apo-enzyme in the presence of various NaCl concentrations. Activation curves indicate that Cl^- binding slightly increases $K_{d,app}$ for the first Ca^{2+} bound. By contrast, Cl^- binding effectively protects α-amylase activity against inhibition by excess of Ca^{2+}. This protection is probably required for optimal activity in the presence of high Ca^{2+} concentrations (~10 mM) in seawater.

TABLE II
Dissociation constants and hydrolytic rate constant computed from substrate (EPS) and chloride saturation curves

The values of the parameters and their standard errors were obtained by fitting the titration data on Equation 3 with a non-linear regression program using the Marquardt-Levenberg algorithm (SigmaPlot 2.0).

Parameter	Constraint	
	$K_d = K'_d$	$K_d \neq K'_d$
K_d (mM)	5.6 ± 0.1	5.3 ± 0.5
K'_d (mM)		5.7 ± 0.1
K'_S (μM)	190 ± 4	193 ± 6
k_2 (s^{-1})	887 ± 6	889 ± 7

Inactivation by Woodward's Reagent K—Carboxyl groups of *A. haloplanctis* α-amylase have been chemically modified by WRK. Fig. 6*A* illustrates the first order inactivation kinetics of *A. haloplanctis* α-amylase. Inactivation by WRK is quite specific to active site residues; nearly complete protection is provided by saturating concentrations of both starch and EPS substrates. As shown in Fig. 6, NaCl also protects α-amylase from WRK inactivation. We found that Cl^-, Br^-, and I^- protect α-amylase to roughly the same extent, whereas SO_4^{2-} does not provide any protection, demonstrating the specific effect of the allosteric effectors. A double reciprocal plot of the pseudo-first order rate constants k_{obs} as a function of WRK concentration (Fig. 6*C*) fails to pass through the origin, indicating the formation of a reversible enzyme-inhibitor complex prior to covalent modification (34, 35). As deduced from this plot, chloride increases the $K_{i,app}$ value of WRK from 4 mM to 8 mM.

Previous data (34) suggest that WRK mainly reacts with the deprotonated form of carboxyl groups (acting as a base during the opening of the isoxazole ring). The protective effect of chloride can be interpreted by an anion-induced alkaline shift of the pK_a of some catalytic groups, therefore becoming less reactive to chemical modification. Protection by steric hindrance cannot be ruled out but nevertheless implies close interactions of Cl^- with the target groups of WRK.

Structure and Engineering of the Chloride Binding Site—The chloride binding site of mammalian pancreatic and salivary α-amylases is composed by Arg-195 ($N^{\eta 2}$,N^{ϵ}), Asn–298 ($N^{\delta 2}$), the side-chain amines of Arg-337 ($N^{\eta 1 \eta 2}$), and a water molecule (4–7). This binding site differs in *A. haloplanctis* by a Lys residue instead of Arg-337 (Fig. 7). Only the basic residue Arg/Lys-337 is substituted in chloride-independent α-amylases. From our sequence alignment, it can be anticipated that α-amylases from *T. curvata*, *Anopheles gambiae*, and *Drosophila melanogaster* also bind a chloride ion. In order to test this

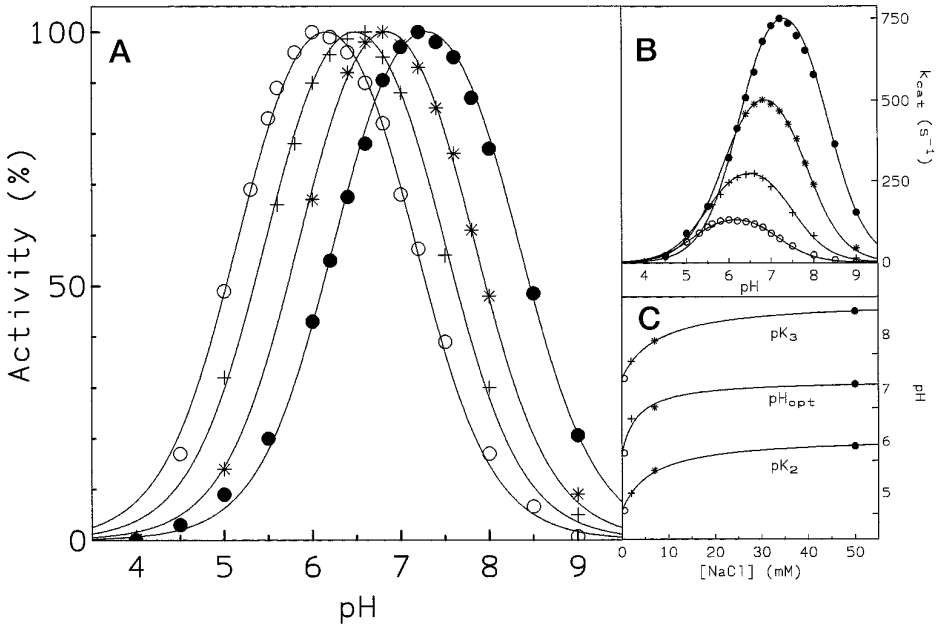

FIG. 4. **pH and chloride dependence of α-amylase activity.** Starch hydrolysis was recorded at various pH levels in the presence of 0.5 mM (○), 2 mM (+), 7 mM (*), and 50 mM (●) NaCl. Amylolytic activity is expressed in % of the maximal k_{cat} (*A*) or by k_{cat} values (*B*). *Solid lines* are theoretical curves calculated from the three-proton model (31, 32). *C*, effect of chloride concentration on pK_2, pK_3, and pH_{opt}. *Solid lines* are theoretical rectangular hyperbola from a binding isotherm.

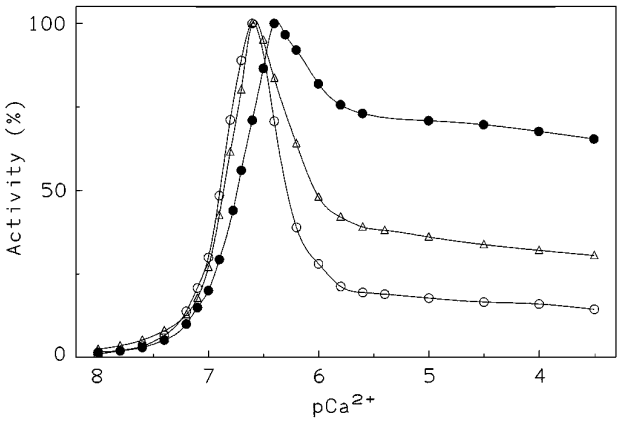

FIG. 5. **Calcium titration of α-amylase activity.** Starch hydrolysis was recorded at increasing free calcium concentrations ($pCa^{2+} = -\log[Ca^{2+}]$) in the presence of 2 mM (○), 7 mM (△), and 50 mM (●) NaCl.

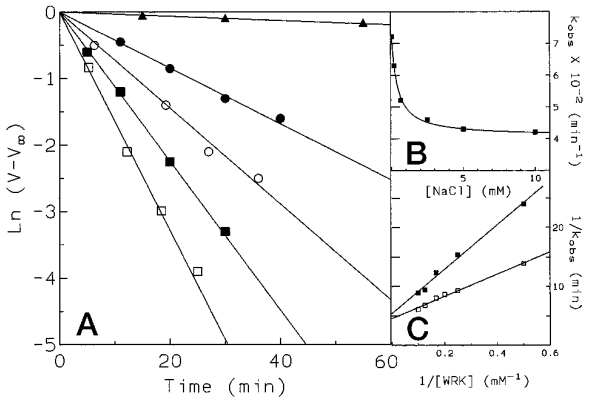

FIG. 6. **Inactivation of α-amylase by WRK.** *A*, semilogarithmic plot of residual activity *versus* time: α-amylase was incubated in the presence of 2 mM WRK (○), 2 mM WRK, 40 mM NaCl (●), 2 mM WRK, 1.6% starch (▲), 10 mM WRK (□), and 10 mM WRK, 40 mM NaCl (■). *B*, concentration dependence of chloride protection. *C*, double-reciprocal plot of k_{obs} as a function of the reagent concentration in absence (□) and in the presence of 40 mM NaCl (■).

hypothesis, α-amylase secreted by the thermophilic actinomycete *T. curvata* was isolated from culture supernatants. This enzyme is indeed activated by chloride and displays K_d values of 7.6 mM at 25 °C and of 2.0 mM at 60 °C.

Table III summarizes the catalytic and binding properties of the recombinant *A. haloplanctis* α-amylase produced in *E. coli* and of its mutant enzymes K337R and K337Q. The mutation of Lys-337 to Arg introduces all the Cl^- ligands of porcine pancreatic α-amylase in the bacterial enzyme but fails to restore the high affinity of the pig enzyme. This mutated α-amylase displays essentially the same kinetic properties as the recombinant non-mutated enzyme, except that the K_d values are at least 10 times higher. It seems that the chloride binding site of *A. haloplanctis* α-amylase cannot accommodate the bulky guanidinium group of an arginine in the appropriate orientation, therefore leading to lower affinity for anions. The mutation Lys-337 to Gln corresponds to the residue organization of Cl^--independent α-amylases from *Bacillus* species (Fig. 7). $^{36}Cl^-$ binding experiments show that this mutant is devoid of a bound chloride ion. Its activity is independent of Cl^-, and the pH_{opt} is strongly shifted toward alkaline values with a $pK_{a,app}$ of 6.6.

DISCUSSION

Structure of the Chloride Binding Site—The protein ligands of Cl^- belong to highly conserved sequence regions of α-amylases (Fig. 7). The ligand Arg-195 is conserved in all starch hydrolases, and Asn-298 is found in almost all α-amylases. These residues are invariably located at the −2 position with respect to the catalytic nucleophile Asp-197 (13) and the essential Asp-300. Only the basic residue Arg/Lys-337 is substituted in chloride-independent α-amylases and therefore appears as an essential component of the site. This is substantiated by the persistence of Cl^- binding in the mutant K337R and mainly by the loss of Cl^- binding ability of the mutant K337Q.

In porcine pancreatic α-amylase, the side chain amine of Arg-337 coordinates the Cl^- ion in a bidentate mode ($N^{\eta 1}\eta 2$) and has a high affinity (K_d = 0.3 mM at 25 °C), whereas lysine in α-amylases from *A. haloplanctis* (K_d = 5.9 mM) and from *T.*

curvata (K_d = 7.6 mM) can only provide a unidentate coordination (N^{ζ}). Comparison of the dissociation constants at 25 °C strongly suggests that the binding affinity is directly related to the chloride coordination mode. Indeed, the two other protein ligands of chloride and the surrounding residues are strictly conserved in the three α-amylases.

Binding of Halides and Other Anions—Activation experiments of *A. haloplanctis* α-amylase by several monovalent anions show that a negative charge, not restricted to that of Cl^-, is essential for the amylolytic reaction. These results also indicate that three main events can be considered separately during activation: (i) the anion binding *per se*, (ii) the pK_a shift of catalytic groups, and (iii) the activation of the amylolytic reaction.

The anion binding site can accommodate ions of various size, however with different affinities. In the case of the monoatomic halides, the decrease of K_d values with ion size (Fig. 1*B*) suggests that optimal van der Waals distances and electrostatic interactions between ion and protein ligands are reached for iodide. It is worth mentioning that the three protein ligands adopt a triangular and nearly equatorial conformation around chloride in the crystal structure (5, 6). One can expect that the strong binding of NO_3^- and ClO_3^-, both having a trigonal configuration, is also the result of optimal ion-ligand contacts. In this respect, the low binding constants displayed by the mutant K337R possibly arise from some distortion in the triangular geometry caused by the guanidinium group. Modeling of the other polyatomic anions within the native site show that coordination distances close to those of Cl^- cannot be provided simultaneously with the three ligands because of the structure and charge distribution of the ionic moieties. Steric hindrance, as exemplified by acetate, also restrict accessibility of larger anions to the site.

All anions tested, with the exception of acetate and F^-, induce the same shift of the optimum pH for activity. It appears that proper shielding of a group involved in anion binding (probably Arg/Lys-337) is required for the pK_a shift of catalytic residues. In addition, the residual activity of the chloride-independent mutant K337Q (whereas the Cl^--free native enzyme is almost inactive) suggests that Arg/Lys-337 inhibits the catalytic mechanism when its positively charged side chain is not neutralized by an anion. On the other hand, there is no clear-cut relation between the activation capacity of the various anions and the K_d values or the pK_a shift (Table I). This discrepancy probably reflects a stringent optimal distance between the anion electron cloud and the enzyme target groups.

	$N^{\eta 2}N^{\varepsilon}$ 195			$N^{\delta 2}$ 298			$N^{\zeta}/N^{\eta 1}\eta^{2}$ 337		
AHA	GVKGF	R	FDASK	VVFVD	N	HDNQR	PYGYP	K	VMSSY
Thecu	GVAGF	R	IDAAK	VVFVV	N	HDTQR	PYGTP	K	VMSSY
PPA	GVAGF	R	LDASK	LVFVD	N	HDNQR	PYGFT	R	VMSSY
Drome	GVAGF	R	VDAAK	LVFVD	N	HDNQR	PFGTP	R	VMSSF
Anoga	GVAGF	R	VDAAK	FVFVD	N	HDNQR	PYGQL	R	IMSSF
Strli	GVDGF	R	IDAAK	AVFVD	N	HDTER	PYGSP	D	VHSGY
Bacam	SLDGF	R	IDAAK	VTFVE	N	HDTQP	ESGYP	Q	VFYGD
Taka	SIDGL	R	IDTVK	GTFVE	N	HDNPR	NDGLP	I	IYAGQ
Barley	GFDAW	R	LDFAR	ATFVD	N	HDTGS	HPGYP	C	IFYDH

FIG. 7. **Alignment of α-amylase homologous regions bearing the chloride ligands.** Protein ligands of the chloride binding site are *boxed* and are *numbered* according to the sequence of PPA. Atoms involved in chloride coordination are also indicated. Active site Asp-197 and Asp-300 are located by *arrows*. Some representative chloride-independent α-amylases are also shown below the line. *AHA*, α-amylases from *A. haloplanctis*; *Thecu*, *T. curvata*; *PPA*, vertebrate pancreas and salivary gland; *Drome*, *D. melanogaster*; *Anoga*, *A. gambiae*; *Strli*, *S. limosus*; *Bacam*, *Bacillus amyloliquefaciens*; *Taka*, *Aspergillus oryzae*; *Barley*, barley seeds. See Ref. 37 for SwissProt and GenBank accession numbers.

Role of the Chloride Effector in α-Amylase—Analysis of substrate and chloride titration curves on the basis of the allosteric activation model (Fig. 3) indicates that the anion effector is not involved in substrate binding but rather in a further catalytic step. The function of the chloride effector has to be interpreted according to the currently accepted reaction mechanism of glycosidases (12, 13, 36) and the crystallographic studies of lysozyme (17), cyclodextrin glycosyltransferase (19), and α-amylase (18). These glycosidases require a protonated side chain acting as a general acid catalyst that would donate a proton to the weakened glycosidic bond. This side chain has been identified as Glu-35 in lysozyme, Glu-257 in CGTase, and Glu-233 in α-amylase. The protonated state of the Glu catalytic residue has been related to local constraints such as the hydrophobic nature of its environment in lysozyme. The following experimental arguments suggest that in chloride-dependent α-amylases, the monovalent anion allows Glu-233 to be protonated at the pH of maximal enzymatic activity (*i.e.* around neutrality). (i) The chloride ion protects *A. haloplanctis* α-amylase from Ca^{2+} inhibition (Fig. 5). An x-ray diffraction study of two *Aspergillus* α-amylases (33) has demonstrated that Ca^{2+} inhibition arises from the binding of a second Ca^{2+} ion to the carboxyl groups of Glu-233 (PPA numbering) in a bidentate mode and of Asp-197 (unidentate mode). Assuming a protonated state of Glu-233 in the presence of Cl^-, it follows that the strength of Ca^{2+} binding (and therefore its inhibitory effect) will be weakened as the Cl^- binding site saturation increases. (ii) The chloride ion protects *A. haloplanctis* α-amylase from WRK inactivation (Fig. 6). These experiments reveal that Cl^- interacts with active site carboxylates; the protective effect is consistent with the appearance of a protonated carboxyl group upon Cl^- binding, which is less prone to WRK modification. (iii) The shift of pH_{opt} and pK_{app}, as well as the concomitant activation following chloride binding (Fig. 4), is well explained by a gradual shift to a more alkaline pK_a of a catalytic group; protonation of Glu-233 would in turn activate the catalytic mechanism.

In pig pancreatic α-amylase, the Cl^- ion is located at 4.8 Å from the protonated side chain of Glu-233, with no shielding group between them (18). Therefore, the monovalent anion is at close proximity of the delta carbon from Glu-233 and can neutralize its δ^+ charge induced by the carbonyl oxygen of the group. Weakening of the OH bond polarization and the resulting pK_a shift toward more alkaline pH values can be expected. Another possibility involves a charge-relay system between chloride, His-299, and Asp-300 (see Fig. 8 in Ref. 18 for a representation of interactions between these residues). There is indeed experimental evidence for the implication of histidyl residues in α-amylase catalysis (31, 32). In the porcine pancreatic α-amylase-acarbose complex, His-299 becomes closely attached to Asp-300, and in CGTase this latter Asp residue has been implicated in the stabilization of the protonated catalytic

TABLE III
Kinetic and binding parameters of the recombinant A. haloplanctis α-amylase (AHAr) and of its mutant enzymes at 25 °C

Enzyme	k_{cat}	K_m	k_{cat}/K_m	$K_{d_{Cl^-}}$	$K_{d_{Br^-}}$	$K_{d_{I^-}}$	Optimum pH	
							$-Cl^-$	$+Cl^-$
	s^{-1}	μM	$s^{-1}\mu M^{-1}$	mM	mM	mM		
AHAr	609 ± 29	168 ± 14	3.62	4.4 ± 0.3	1.7 ± 0.1	1.3 ± 0.1	6.2	7.4
K337R	338 ± 39	131 ± 13	2.58	44 ± 3.8	27 ± 1.8	24 ± 3.4	6.4	7.2
K337Q	77 ± 4	89 ± 7	0.86				7.6	7.6

carboxyl group (19). His-299 is the closest histidyl from Cl^- (5.1 Å) to which it is H-bonded via a water molecule; a charge relay system between Cl^- and Asp-300 would assist the latter in shifting the pK_a of Glu-233.

One should note that most microbial and plant α-amylases are Cl^- independent and have acidic optimum pH values. Chloride binding can provide two advantages: it shifts pH_{opt} to values close to that of the physiological environment and it dramatically increases the specific activity of this specialized α-amylase family.

Acknowledgments—We acknowledge the "Expeditions Polaires Françaises" for the support and facilities offered at the Antarctic station Dumont d'Urville during earlier stages of this work. We are grateful to Prof. J. M. Frère for helpful discussions. We also thank Z. Manco, N. Gerardin-Otthiers, and R. Marchand for expert technical assistance.

REFERENCES

1. Thoma, J. A., Spradlin, J. E., and Dygert, S. (1971) in *The Enzymes* (Boyer, P. D., ed) 3rd Ed., Vol. 5, pp. 115–189, Academic Press, Inc., New York
2. Brady, R. L., Brzozowsi, A. M., Derewenda, Z. S., Dodson, E. J., and Dodson, G. G. (1991) *Acta Crystallogr.* **47,** 527–535
3. Swift, H. J., Brady, L., Derewenda, Z. S., Dodson, E. J., Dodson, G. G., Turkenburg, J. P., and Wilkinson, A. J. (1991) *Acta Crystallogr.* **47,** 535–544
4. Brayer, G. D., Luo, Y., and Withers, S. (1995) *Protein Sci.* **4,** 1730–1742
5. Qian, M., Haser, R., and Payan, F. (1993) *J. Mol. Biol.* **231,** 785–799
6. Larson, S. B., Greenwood, A., Cascio, D., Day, J., and McPherson, A. (1994) *J. Mol. Biol.* **235,** 1560–1584
7. Ramasubbu, N., Paloth, V., Luo, Y., Brayer, G. D., and Levine, M. J. (1996) *Acta Crystallogr.* **52,** 435–446
8. Kadziola, A., Abe, J., Svensson, B., and Haser, R. (1994) *J. Mol. Biol.* **239,** 104–121
9. Machius, M., Wiegand, G., and Huber, R. (1995) *J. Mol. Biol.* **246,** 545–559
10. Bush, D. S., Sticher, L., van Huystee, R., Wagner, D., and Jones, R. L. (1989) *J. Biol. Chem.* **264,** 19392–19398
11. Violet, M., and Meunier, J. C. (1989) *Biochem. J.* **263,** 665–670
12. McCarter, J. D., and Withers, S. G. (1994) *Curr. Opin. Struct. Biol.* **4,** 885–892
13. McCarter, J. D., and Withers, S. G. (1996) *J. Biol. Chem.* **271,** 6889–6894
14. Svensson, B. (1994) *Plant Mol. Biol.* **25,** 141–157
15. Tao, B. Y., Reilly, P. J., and Robyt, J. F. (1989) *Biochim. Biophys. Acta* **995,** 214–220
16. Sinnot, M. L. (1990) *Chem. Rev.* **90,** 1171–1202
17. Strynadka, N. C., and James, M. G. (1991) *J. Mol. Biol.* **220,** 401–424
18. Qian, M., Haser, R., Buisson, G., Duée, E., and Payan, F. (1994) *Biochemistry* **33,** 6284–6294
19. Strokopytov, B., Penninga, D., Rozeboom, H. J., Kalk, K. H., Dijkhuizen, L., and Dijkstra, B. W. (1995) *Biochemistry* **34,** 2234–2240
20. Levitzki, A., and Steer, M. L. (1974) *Eur. J. Biochem.* **41,** 171–180
21. Lifshitz, R., and Levitzki, A. (1976) *Biochemistry* **15,** 1987–1993
22. Feller, G., Lonhienne, T., Deroanne, C., Libioulle, C., Van Beeumen, J., and Gerday, C. (1992) *J. Biol. Chem.* **267,** 5217–5221
23. Feller, G., Payan, F., Theys, F., Qian, M., Haser, R., and Gerday, C. (1994) *Eur. J. Biochem.* **222,** 441–447
24. Vihinen, M., and Mäntsälä, P. (1989) *Crit. Rev. Biochem. Mol. Biol.* **24,** 329–418
25. Rauscher, E., Neumann, U., Schaich, E., von Bülow, S., and Wahlefeld, A. W. (1985) *Clin. Chem.* **31,** 14–19
26. Bernfeld, P. (1955) *Methods Enzymol.* **1,** 149–151
27. Robertson, S. P., Potter, J. D., and Rouslin, W. (1982) *J. Biol. Chem.* **257,** 1743–1748
28. Levy, H. M., Leber, P. D., and Ryan, E. M. (1963) *J. Biol. Chem.* **238,** 3654–3659
29. Hensley, A., Arnheim, N., Toney, M. D., Cortopassi, G., and Galas, D. (1989) *Nucleic Acids Res.* **17,** 6545–6551
30. Cease, K. B., Potcova, C. A., Lohff, C. J., and Zeigler, M. E. (1994) *PCR Methods Appl.* **3,** 298–300
31. Ishikawa, K., Matsui, I., and Honda, K. (1990) *Biochemistry* **29,** 7119–7123
32. Ishikawa, K., Matsui, I., Kobayashi, S., Nakatani, H., and Honda, K. (1993) *Biochemistry* **32,** 6259–6265
33. Boel, E., Brady, L., Brzozowsi, A. M., Derewenda, Z., Dodson, G. G., Jensen, V. J., Petersen, S. B., Swift, H., Thim, L., and Woldike, H. F. (1990) *Biochemistry* **29,** 6244–6249
34. Petra, P. H. (1971) *Biochemistry* **10,** 3163–3170
35. Brake, A. J., and Weber, B. H. (1974) *J. Biol. Chem.* **249,** 5452–5457
36. Mooser, G. (1992) in *The Enzymes* (Sigman, D. S., ed) 3rd Ed., Vol. 20, pp. 187–233, Academic Press, Inc., New York
37. Janecek, S. (1994) *Eur. J. Biochem.* **224,** 519–524